Higgs decay to light (pseudo)scalars in the semi-constrained NMSSM*

Shiquan Ma(马士全)[1] Kun Wang(王坤)[1] Jingya Zhu(朱经亚)[1,2†]

[1]Center for Theoretical Physics, School of Physics and Technology, Wuhan University, Wuhan 430072, China
[2]School of Physics and Electronics, Henan University, Kaifeng 475004, China

Abstract: The next-to minimal supersymmetric standard model (NMSSM) with non-universal Higgs masses, i.e., the semi-constrained NMSSM (scNMSSM), extends the minimal supersymmetric standard model (MSSM) by a singlet superfield and assumes universal conditions, except for the Higgs sector. It can not only maintain the simplicity and grace of the fully constrained MSSM and NMSSM and relieve the tension they have been facing since the discovery of the 125-GeV Higgs boson but also allow for an exotic phenomenon wherein the Higgs decay into a pair of light (10 ~ 60 GeV) singlet-dominated (pseudo)scalars (hereafter, in this paper, we use "scalar" for both scalars and pseudoscalars, considering pseudoscalars can also be called *CP*-odd scalars). This condition can be classified into three scenarios according to the identitiesof the SM-like Higgs and the light scalar: (i) the light scalar is *CP*-odd, and the SM-like Higgs is h_2; (ii) the light scalar is *CP*-odd, and the SM-like Higgs is h_1; and (iii) the light scalar is *CP*-even, and the SM-like Higgs is h_2. In this work, we compare the three scenarios, checking the interesting parameter regions that lead to the scenarios, the mixing levels of the doublets and singlets, the tri-scalar coupling between the SM-like Higgs and a pair of light scalars, the branching ratio of Higgs decay to the light scalars, and sensitivities in the detection of the exotic decay at the HL-LHC and future lepton colliders such as CEPC, FCC-ee, and ILC. Finally, several interesting conclusions are drawn, which are useful for understanding the different delicate mechanisms of the exotic decay and designing colliders in future.

Keywords: Higgs, supersymmetry phenomenology, NMSSM

DOI: 10.1088/1674-1137/abce4f

I. INTRODUCTION

In 2012, a new boson of approximately 125 GeV was discovered at the LHC [1,2], which in later years, was consistently verified to be the SM-like Higgs boson with an increasing amount of data [3-7]. However, some other questions still exist, e.g., whether another scalar survives in the low mass region, and whether there is exotic Higgs decay into light scalars. Before the LHC, for the low integrated luminosity (IL), the LEP did not exclude a light scalar with a smaller production rate than the SM-like Higgs [8]. The CMS(ATLAS) collaboration searched for resonances directly in the $bj\mu\mu$ channel in the 10~60 (20~70) GeV range [9,10]. The two collaborations also searched for the exotic Higgs decay to light resonances in final states with $b\bar{b}\tau^+\tau^-$ [11], $b\bar{b}\mu^+\mu^-$ [12,13], $\mu^+\mu^-\tau^+\tau^-$ [14-16], 4τ [16,17], 4μ [18-20], $4b$ [21], $\gamma\gamma gg$ [22], and 4γ [23]. However, there is still sufficient space left for physics on the exotic decay. For example, in the $b\bar{b}\tau^+\tau^-$ channel reported by CMS collaboration [11], the 95% exclusion limit is at least 3% in the 20 ~ 60 GeV region. According to simulations, however, the future limits could be 0.3% at the High-Luminosity program of the Large Hadron Collider (HL-LHC) [24], 0.04% at the Circular Electron Positron Collider (CEPC), and 0.02% at the Future Circular Colliders in e^+e^- collisions (FCC-ee) [25, 26].

This exotic Higgs decay to light scalars can be investigated via many theories beyond the Standard Model (BSM) [27], e.g., the next-to minimal supersymmetric standard model (NMSSM), the simplest little Higgs model, the minimal dilaton model, the two-Higgs-doublet model, the next-to two-Higgs-doublet model, the singlet extension of the SM, etc. Several phenomenological studies on the exotic decay exist with these models [28-42].

The NMSSM extends the MSSM by a singlet superfield $\hat{S}$, thereby solving the μ-problem and relaxing the fine-tuning tension resulting from the discovery of the

Received 24 August 2020; Accepted 20 November 2020; Published online 28 December 2020
* Supported by National Natural Science Foundation of China (NSFC) (11605123)
† E-mail: zhujy@whu.edu.cn

Higgs in 2012 [43-49]. However, as supersymmetric (SUSY) models, the MSSM and NMSSM both suffer from a huge parameter space of over 100 dimensions. In most studies, some parameters are manually assumed equal at low-energy scales, leaving only about 10 free parameters, without considering the Renormalization Group Equations (RGEs) running from high scales [43-49]. In Ref. [33], decay of a Higgs boson of 125 GeV into light scalars was studied in the NMSSM with parameters set in this way. In contrast, in constrained models, congeneric parameters are assumed universal at the Grand Unified Theoretical (GUT) scale, leaving only four free parameters in the fully-constrained MSSM (CMSSM) and four or five in the fully-constrained NMSSM (CNMSSM) [50-57]. However, it was found that CMSSM and CNMSSM were nearly excluded considering the 125 GeV Higgs data, high mass bounds of gluino and squarks in the first two generations, muon g-2, and dark matter relic density and detections [56-62].

The semi-constrained NMSSM (scNMSSM) relaxes the unified conditions of the Higgs sector at the GUT scale; thus, it is also called the NMSSM with non-universal Higgs mass (NUHM) [63-66]. It not only keeps the simplicity and grace of the CMSSM and CNMSSM but also relaxes the tension that they have faced since the discovery of SM-like Higgs [67]. Moreover, it makes predictions about interesting light particles such as a singlino-like neutralino [68] and light Higgsino-dominated NLSPs [69-71]. In this work, we study the scenarios in the scNMSSM with a light scalar of $10\sim 60$ GeV and the detections of exotic Higgs decay to a pair of it.

The main points of this paper are listed as follows. In Sec. II, we introduce the model briefly and provide some related analytic formulas. In Sec. III, we present in detail the numerical calculations and discussions. Finally, we draw our conclusions in Sec. IV.

II. THE MODEL AND ANALYTIC CALCULATIONS

The superpotential of NMSSM, with $\mathbb{Z}_3$ symmetry, is written as [72]

$$W = W_{\rm Yuk} + \lambda\hat{S}\,\hat{H}_u\cdot\hat{H}_d + \frac{1}{3}\kappa\hat{S}^3\,, \tag{1}$$

from which the so-called F-terms of the Higgs potential can be derived as

$$V_{\rm F} = |\lambda S|^2(|H_u|^2+|H_d|^2) + |\lambda H_u\cdot H_d + \kappa S^2|^2\,. \tag{2}$$

The D-terms are the same as in the MSSM

$$V_{\rm D} = \frac{1}{8}\left(g_1^2+g_2^2\right)\left(|H_d|^2-|H_u|^2\right)^2 + \frac{1}{2}g_2^2\left|H_u^\dagger H_d\right|^2\,, \tag{3}$$

where g_1 and g_2 are the gauge couplings of $U(1)_Y$ and $SU(2)_L$, respectively. Without considering the SUSY-breaking mechanism, at a low-energy scale, the soft-breaking terms can be imposed manually to the Lagrangian. In the Higgs sector, these terms corresponding to the superpotential are

$$\begin{aligned} V_{\rm soft} =& M_{H_u}^2|H_u|^2 + M_{H_d}^2|H_d|^2 + M_S^2|S|^2 \\ &+\left(\lambda A_\lambda S\,H_u\cdot H_d + \frac{1}{3}\kappa A_\kappa S^3 + {\rm h.c.}\right), \end{aligned} \tag{4}$$

where $M_{H_u}^2, M_{H_u}^2, M_S^2$ are the soft masses of Higgs fields H_u, H_d, S, respectively, and A_λ, A_κ are the trilinear couplings at the $M_{\rm SUSY}$ scale. However, in the scNMSSM, the SUSY breaking is mediated by gravity; thus, the soft-parameters at the $M_{\rm SUSY}$ scale are running naturally from the GUT scale complying with the RGEs.

At electroweak symmetry breaking, H_u, H_d, and S get their vacuum expectation values (VEVs) v_u, v_d, and v_s, respectively, with $\tan\beta\equiv v_u/v_d$, $v\equiv\sqrt{v_u^2+v_d^2}\approx$ 174 GeV, and $\mu_{\rm eff}\equiv\lambda v_s$. Then, they can be written as

$$\begin{aligned} H_u &= \begin{pmatrix} H_u^+ \\ v_u+\dfrac{\phi_1+{\rm i}\varphi_1}{\sqrt{2}} \end{pmatrix}, \\ H_d &= \begin{pmatrix} v_d+\dfrac{\phi_2+{\rm i}\varphi_2}{\sqrt{2}} \\ H_d^- \end{pmatrix}, \\ S &= v_s+\frac{\phi_3+{\rm i}\varphi_3}{\sqrt{2}}. \end{aligned} \tag{5}$$

The Lagrangian consists of the F-terms, D-terms, and soft-breaking terms; therefore, with the above equations, one can get the tree-level squared-mass matrix of CP-even Higgses in the base $\{\phi_1,\phi_2,\phi_3\}$ and CP-odd Higgses in the base $\{\varphi_1,\varphi_2,\varphi_3\}$ [72]. After diagonalizing the mass squared matrixes including loop corrections [73], one can get the mass-eigenstate Higgses (three CP-even ones $h_{1,2,3}$ and two CP-odd ones $a_{1,2}$, in mass order) from the gauge-eigenstate ones ($\phi_{1,2,3}$ and $\varphi_{1,2,3}$ in Eq. (5), with $1,2,3$ corresponding to up-type, down-type, and singlet states, respectively):

$$h_i = S_{ik}\phi_k, \quad a_j = P_{jk}\varphi_k\,, \tag{6}$$

where S_{ik}, P_{jk} are the corresponding components of ϕ_k in h_i and φ_k in a_j, respectively, with $i,k=1,2,3$ and $j=1,2$.

In the scNMSSM, the SM-like Higgs (hereafter, uniformly denoted as h) can be CP-even h_1 or h_2, and the light scalar (hereafter uniformly denoted as s) can be CP-odd a_1 or CP-even h_1. Then, the couplings between the SM-like Higgs and a pair of light scalars C_{hss} can be written at tree level as [74]

$$
\begin{aligned}
C^{\rm tree}_{h_2h_1h_1} =& \frac{\lambda^2}{\sqrt{2}}\left[v_u\left(\Pi^{122}_{211}+\Pi^{133}_{211}\right)\right.\\
&\left.+v_d\left(\Pi^{211}_{211}+\Pi^{233}_{211}\right)+v_s\left(\Pi^{311}_{211}+\Pi^{322}_{211}\right)\right]\\
&-\frac{\lambda\kappa}{\sqrt{2}}\left(v_u\Pi^{323}_{211}+v_d\Pi^{313}_{211}+2v_s\Pi^{123}_{211}\right)\\
&+\sqrt{2}\kappa^2 v_s\Pi^{333}_{211}-\frac{\lambda A_\lambda}{\sqrt{2}}\Pi^{123}_{211}+\frac{\kappa A_\kappa}{3\sqrt{2}}\Pi^{333}_{211}\\
&+\frac{g^2}{2\sqrt{2}}\left[v_u\left(\Pi^{111}_{211}-\Pi^{122}_{211}\right)-v_d\left(\Pi^{211}_{211}-\Pi^{222}_{211}\right)\right], \quad (7)
\end{aligned}
$$

where

$$\Pi^{ijk}_{211}=2S_{2i}S_{1j}S_{1k}+2S_{1i}S_{2j}S_{1k}+2S_{1i}S_{1j}S_{2k};$$

or

$$
\begin{aligned}
C^{\rm tree}_{h_a a_1 a_1} =& \frac{\lambda^2}{\sqrt{2}}\left[v_u\left(\Pi^{122}_{a11}+\Pi^{133}_{a11}\right)\right.\\
&\left.+v_d\left(\Pi^{211}_{a11}+\Pi^{233}_{a11}\right)+v_s\left(\Pi^{311}_{a11}+\Pi^{322}_{a11}\right)\right]\\
&+\frac{\lambda\kappa}{\sqrt{2}}\left[v_u\left(\Pi^{233}_{a11}-2\Pi^{323}_{a11}\right)+v_d\left(\Pi^{133}_{a11}-2\Pi^{313}_{a11}\right)\right.\\
&\left.+2v_s\left(\Pi^{312}_{a11}-\Pi^{123}_{a11}-\Pi^{213}_{a11}\right)\right]+\sqrt{2}\kappa^2 v_s\Pi^{333}_{a11}\\
&+\frac{\lambda A_\lambda}{\sqrt{2}}\left(\Pi^{123}_{a11}+\Pi^{213}_{a11}+\Pi^{312}_{a11}\right)-\frac{\kappa A_\kappa}{3\sqrt{2}}\Pi^{333}_{a11}\\
&+\frac{g^2}{2\sqrt{2}}\left[v_u\left(\Pi^{111}_{a11}-\Pi^{122}_{a11}\right)-v_d\left(\Pi^{211}_{a11}-\Pi^{222}_{a11}\right)\right], \quad (8)
\end{aligned}
$$

where $\Pi^{ijk}_{a11}=2S_{ai}P_{1j}P_{1k}$, and $a=1,2$. Thus, the width of Higgs decay to a pair of light scalars can be given by

$$\Gamma(h\to ss)=\frac{1}{32\pi m_h}C^2_{hss}\left(1-\frac{4m_s^2}{m_h^2}\right)^{1/2}. \quad (9)$$

Then, the light scalars decay to light SM particles, such as a pair of light quarks or leptons, gluons, or photons. The widths of light scalar decay to quarks and charged leptons at tree level are given by

$$\Gamma(s\to l^+l^-)=\frac{\sqrt{2}G_F}{8\pi}m_s m_l^2\left(1-\frac{4m_l^2}{m_s^2}\right)^{p/2}, \quad (10)$$

$$\Gamma(s\to q\bar{q})=\frac{N_c G_F}{4\sqrt{2}\pi}C^2_{sqq}m_s m_q^2\left(1-\frac{4m_q^2}{m_s^2}\right)^{p/2}, \quad (11)$$

where $p=1$ for CP-odd s, and $p=3$ for CP-even s. The couplings between light scalar and up-type or down-type quarks are given by

$$C_{h_1 t_L t_R^c}=\frac{m_t}{\sqrt{2}v\sin\beta}S_{11}, \quad (12)$$

$$C_{h_1 b_L b_R^c}=\frac{m_b}{\sqrt{2}v\cos\beta}S_{12}, \quad (13)$$

$$C_{a_1 t_L t_R^c}=\mathrm{i}\frac{m_t}{\sqrt{2}v\sin\beta}P_{11}, \quad (14)$$

$$C_{a_1 b_L b_R^c}=\mathrm{i}\frac{m_b}{\sqrt{2}v\cos\beta}P_{12}. \quad (15)$$

III. NUMERICAL CALCULATIONS AND DISCUSSIONS

In this work, we first scan the following parameter space with NMSSMTOOLS-5.5.2 [74,75]:

$$
\begin{aligned}
&0<\lambda<0.7, \quad 0<\kappa<0.7, \quad 1<\tan\beta<30,\\
&100<\mu_{\rm eff}<200\ \text{GeV}, \quad 0<M_0<500\ \text{GeV},\\
&0.5<M_{1/2}<2\ \text{TeV}, \quad |A_0|, |A_\lambda|, |A_\kappa|<10\ \text{TeV}, \quad (16)
\end{aligned}
$$

where we choose small $\mu_{\rm eff}$ to get low fine tuning, small M_0 to get large muon g-2, and moderate $M_{1/2}$ to meet both large muon g-2 and high gluino-mass bounds. The regions of other parameters are chosen to be wide to investigate all scenarios with a low mass scalar and the exotic Higgs decay.

The constraints we imposed in our scan include the following: (i) an SM-like Higgs of 123~127 GeV, with signal strengths and couplings satisfying the current Higgs data [3-7]; (ii) search results for exotic and invisible decay of the SM-like Higgs, and Higgs-like resonances in other mass regions, with HIGGSBOUNDS-5.7.1 [76-78]; (iii) the muon g-2 constraint, like that in Ref. [67]; (iv) the mass bounds of gluino and the first-two-generation squarks over 2 TeVand search results for electroweakinos in multilepton channels [79]; (vi) the dark matter relic density Ωh^2 below 0.131 [80], and the dark matter and nucleon scattering cross section below the upper limits in direct searches [81,82]; and (vii) the theoretical constraints of vacuum stability and Landau pole.

After imposing these constraints, the surviving samples can be categorized into three scenarios:

• Scenario I: h_2 is the SM-like Higgs, and the light scalar a_1 is CP-odd;

• Scenario II: h_1 is the SM-like Higgs, and the light scalar a_1 is CP-odd;

• Scenario III: h_2 is the SM-like Higgs, and the light scalar h_1 is CP-even.

In Table 1, we list the ranges of parameters and light particle masses in the three scenarios. From the table, one can see that the parameter ranges are nearly the same except for λ, κ, and A_κ, but the mass spectrums for light

Table 1. The ranges of parameters and light particle masses in Scenario I, II, and III.

	Scenario I	Scenario II	Scenario III
λ	$0\sim0.58$	$0\sim0.24$	$0\sim0.57$
κ	$0\sim0.21$	$0\sim0.67$	$0\sim0.36$
$\tan\beta$	$14\sim27$	$10\sim28$	$13\sim28$
$\mu_{\rm eff}$/GeV	$103\sim200$	$102\sim200$	$102\sim200$
M_0 /GeV	$0\sim500$	$0\sim500$	$0\sim500$
$M_{1/2}$/TeV	$1.06\sim1.47$	$1.04\sim1.44$	$1.05\sim1.47$
A_0/TeV	$-2.8\sim0.2$	$-3.2\sim-1.0$	$-2.8\sim0.6$
$A_\lambda(M_{\rm GUT})$/TeV	$1.3\sim9.4$	$0.1\sim10$	$1.1\sim9.8$
$A_\kappa(M_{\rm GUT})$/TeV	$-0.02\sim5.4$	$-0.02\sim0.9$	$-0.7\sim5.7$
$A_\lambda(M_{\rm SUSY})$/TeV	$2.0\sim10.1$	$0.8\sim10.9$	$1.6\sim10.2$
$A_\kappa(M_{\rm SUSY})$/GeV	$-51\sim42$	$-17\sim7$	$-803\sim11$
$m_{\tilde{\chi}_1^0}$/GeV	$3\sim129$	$98\sim198$	$3\sim190$
m_{h_1}/GeV	$4\sim123$	$123\sim127$	$4\sim60$
m_{h_2}/GeV	$123\sim127$	$127\sim5058$	$123\sim127$
m_{a_1}/GeV	$4\sim60$	$0.5\sim60$	$3\sim697$

particles are totally different.

To study the different mechanisms of Higgs decay to light scalars in different scenarios, we recombine relevant parameters and show them in Fig. 1. From this figure, one can find the following:

• For Scenarios I and III, $\lambda A_\lambda S_{22}\approx\lambda^2 v_s$, where $0.03\lesssim S_{22}\lesssim0.07$ is at the same order with $1/\tan\beta$, for the mass scale of the *CP*-odd doublet scalar $M_A\sim2\mu_{\rm eff}/\sin2\beta\sim A_\lambda\gg\kappa v_s$, and $\tan\beta\gg1$ [33]. Thus, the SM-like Higgs is up-type-doublet dominated.

• For Scenario I, κA_κ, $k^2 v_s$, and $\lambda\kappa v_s$ are at the same level of a few GeV; however, for Scenario II, $\kappa^2 v_s$ can be as large as a few TeV for small λ and large κ.

• Especially, for Scenario III, $\kappa A_\kappa\approx-4\kappa^2 v_s$, or $A_\kappa\approx-4\kappa v_s$.

According to the large data of the 125 GeV Higgs and current null results searching for non-SM Higgs, the 125 GeV Higgs should be doublet dominated, and the light scalar should be singlet dominated. In our cases, we found that, in the *CP*-even sector, the mixing between singlet and up-type doublet η_{us}, the mixing between down-type doublet and up-type doublet η_{ud}, and the mixing between singlet and down-type doublet η_{ds} are, respectively, roughly equal to

$$\eta_{us}\approx\frac{2\lambda v\mu_{\rm eff}\left[1-\left(\dfrac{M_A}{2\mu/\sin2\beta}\right)^2-\dfrac{\kappa}{2\lambda}\sin2\beta\right]}{m_h^2-m_s^2},$$
$$\eta_{ud}\approx\frac{1}{\tan\beta},$$
$$\eta_{ds}\approx-\frac{\eta_{us}}{\tan\beta},\qquad(17)$$

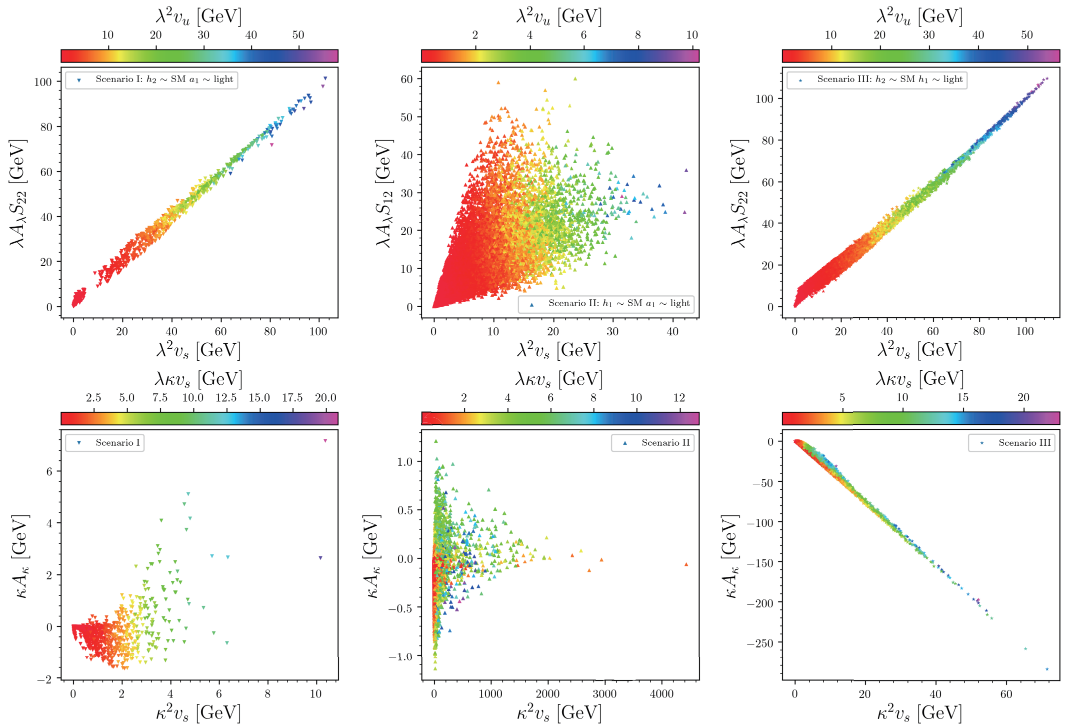

Fig. 1. (color online) Surviving samples for the three scenarios in the $\lambda A_\lambda S_{i2}$ versus $\lambda^2 v_s$ (upper), where S_{22} (left and right) and S_{12} (middle) are the down-type-doublet component coefficient in the SM-like Higgs, and κA_κ versus $\kappa^2 v_s$ (lower) planes, respectively. Colors indicate $\lambda^2 v_u$ (upper) and $\lambda\kappa v_s$ (lower), respectively.

where m_h and m_s are masses of the SM-like Higgs and the singlet-dominated *CP*-even scalar, respectively, and

$$|\eta_{ds}| \ll |\eta_{us}|, |\eta_{ud}| \ll 1 . \tag{18}$$

And in the *CP*-odd sector, the mixing between singlet and down-type doublet η'_{ds}, the mixing between down-type doublet and up-type doublet η'_{ud}, and the mixing between singlet and up-type doublet η'_{us} are, respectively, roughly equal to

$$\eta'_{ds} \approx \frac{\lambda v \dfrac{M_A^2}{2\mu_{\rm eff}/\sin 2\beta} - 3\kappa v \mu_{\rm eff}}{m_{a_2}^2 - m_{a_1}^2} \approx \frac{\lambda v}{\mu_{\rm eff}\tan\beta},$$
$$\eta'_{ud} \approx \frac{1}{\tan\beta},$$
$$\eta'_{us} \approx -\frac{\eta'_{ds}}{\tan\beta}, \tag{19}$$

where

$$|\eta'_{us}| \ll |\eta'_{ds}|, |\eta'_{ud}| \ll 1 . \tag{20}$$

Specifically, in Scenario I,

$$S_{23} = \eta_{us}, \quad S_{22} = \eta_{ud}, \quad P_{11} = \eta'_{us}, \quad P_{12} = \eta'_{ds}; \tag{21}$$

in Scenario II,

$$S_{13} = \eta_{us}, \quad S_{12} = \eta_{ud}, \quad P_{11} = \eta'_{us}, \quad P_{12} = \eta'_{ds}; \tag{22}$$

in Scenario III,

$$S_{23} = \eta_{us}, \quad S_{22} = \eta_{ud}, \quad S_{11} = -\eta_{us}, \quad S_{12} = \eta_{ds}. \tag{23}$$

In Fig. 2, we show how small they can be and their relative scale. From this figure, we can see the following for the three scenarios.

• Scenario I: The up-type-doublet component of the light scalar, $-0.0015 \lesssim P_{11} < 0$, is proportional to the parameter λ; thus, the total doublet component of the light scalar is $P_{1D} \equiv \sqrt{P_{11}^2 + P_{12}^2} \approx P_{11}\tan\beta \lesssim 0.04$, while the singlet component of the SM-like Higgs is $|S_{23}| \lesssim 0.3$.

• Scenario II: The up-type-doublet component of the light scalar, $-0.0006 \lesssim P_{11} < 0$, is proportional to the parameter λ; thus, the total doublet component of the light scalar is $0 < P_{1D} \lesssim 0.013$, while the singlet component in the SM-like Higgs is $|S_{13}| \lesssim 0.3$.

• Scenario III: The up-type-doublet component of the light scalar and the singlet component of the SM-like Higgs are anticorrelated, i.e., $S_{11} \approx -S_{23}$, and their range is $-0.15 \lesssim S_{11} \lesssim 0.2$, with the sign related to the parameter λ. This also means that the mixing in the *CP*-even scalar sector is mainly between the singlet and the up-type doublet, and we found that $0.03 \lesssim S_{22} \lesssim 0.07$ and $S_{12} \lesssim 0.03$. Thus, the SM-like Higgs is up-type doublet dominated, which is applicable in all three scenarios, with $S_{21} \approx 1$ in Scenario I and III and $S_{11} \approx 1$ in Scenario II.

Considering the values of and correlations among parameters and component coefficients, the couplings between the SM-like Higgs and a pair of light scalars can be simplified as

$$C_{h_2 a_1 a_1} \simeq \sqrt{2}\lambda^2 v_u + \sqrt{2}\lambda A_\lambda P_{11}\tan\beta, \tag{24}$$

$$C_{h_1 a_1 a_1} \simeq \sqrt{2}\lambda^2 v_u + \sqrt{2}\lambda A_\lambda P_{11}\tan\beta + 2\sqrt{2}\kappa^2 v_s S_{13}, \tag{25}$$

$$C_{h_2 h_1 h_1} \simeq \sqrt{2}\lambda^2 v_u - \sqrt{2}\lambda A_\lambda S_{12} + \sqrt{2}\lambda^2 v_s S_{11}$$
$$+ 2\sqrt{2}\kappa^2 v_s S_{23} + \frac{3g^2}{\sqrt{2}} v_u S_{11} S_{11}$$
$$- 2\sqrt{2}\lambda\kappa v_s S_{12}. \tag{26}$$

In Fig. 3, we show the exotic branching ratio $Br(h \to ss)$ including one-loop correction correlated with the mass of the light scalar and the coupling between the SM-like

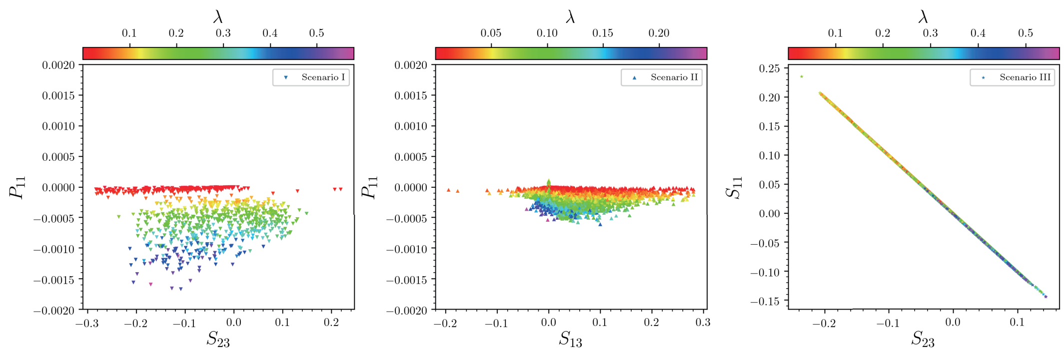

Fig. 2. (color online) Surviving samples for the three scenarios in the P_{11} versus S_{23} (left), P_{11} versus S_{13} (middle), and S_{11} versus S_{23} (right) planes, respectively, where S_{23} (left and right) and S_{13} (middle) are the singlet component in the SM-like Higgs, and P_{11} (left and middle) and S_{11} (right) are the up-type-doublet components of the light scalar, respectively. Colors indicate the parameter λ.

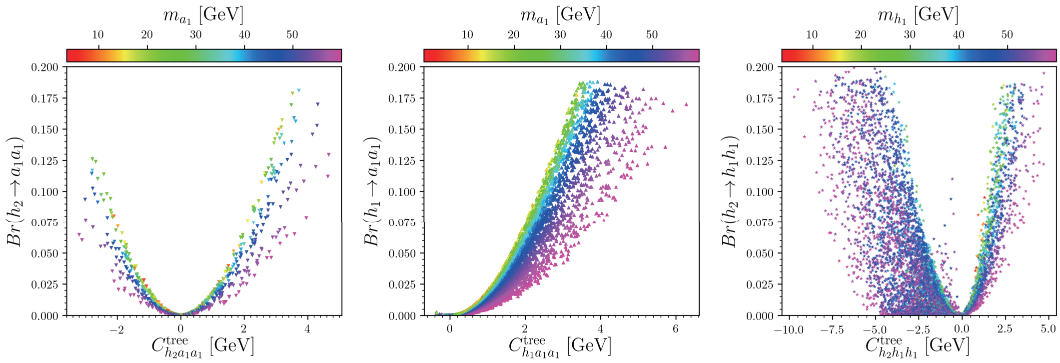

Fig. 3. (color online) Surviving samples for the three scenarios in the exotic branching ratio $Br(h\to ss)$ versus the tri-scalar coupling $C^{\rm tree}_{hss}$ at tree level planes, respectively, with colors indicating the mass of light Higgs m_s, where h denotes the SM-like Higgs h_2 (left and right) and h_1 (middle), and s denotes the light scalar a_1 (left and middle) and h_1 (right).

Higgs and a pair of the light scalars at tree level. Since the 125 GeV Higgs is constrained to be very SM-like, its decay widths and branching ratios to SM particles cannot vary much, which leads indirectly to strong upper limits on exotic branching ratios of the SM-like Higgs [3-5][1)]. Thus, combined with Eq. (9), it is natural that the branching ratios to light scalars are proportional to the square of the tri-scalar couplings. The significant deviations for the negative-coupling samples in Scenario III are because of the one-loop correction of the stop loops,

$$\Delta C_{h_2h_1h_1} \simeq S_{21}S_{11}^2\frac{3\sqrt{2}m_t^4}{16\pi^2v_u^3}\ln\left(\frac{m_{\tilde{t}_1}m_{\tilde{t}_2}}{m_t^2}\right), \tag{27}$$

which can be as large as 5 GeV, whereas for Scenario I and II, they are

$$\Delta C_{h_2a_1a_1} \simeq S_{21}P_{11}^2\frac{3\sqrt{2}m_t^4}{16\pi^2v_u^3}\ln\left(\frac{m_{\tilde{t}_1}m_{\tilde{t}_2}}{m_t^2}\right), \tag{28}$$

$$\Delta C_{h_1a_1a_1} \simeq S_{11}P_{11}^2\frac{3\sqrt{2}m_t^4}{16\pi^2v_u^3}\ln\left(\frac{m_{\tilde{t}_1}m_{\tilde{t}_2}}{m_t^2}\right). \tag{29}$$

Since $P_{11}\ll S_{11}$, as seen from Fig. 2, the loop correction in Scenarios I and II is much smaller than that in Scenario III. In the following figures and discussions, we consider the coupling C_{hss} to include the one-loop correction ΔC_{hss}, unless otherwise specified.

A. Detections at the HL-LHC

At the LHC, the SM-like Higgs can first be produced in gluon fusion (ggF), vector boson fusion (VBF), associated with vector boson (Wh, Zh), or associated with $t\bar{t}$ processes, where the cross section in the ggF process is much larger than that of others. Then, the SM-like Higgs can decay to a pair of light scalars, and each scalar can then decay to a pair of fermions, gluons, or photons. The ATLAS and CMS collaborations have searched for these exotic decay modes in the final states of $b\bar{b}\tau^+\tau^-$ [11], $b\bar{b}\mu^+\mu^-$ [12,13], $\mu^+\mu^-\tau^+\tau^-$ [14-16], 4τ [16,17], 4μ [18-20], $4b$ [21], $\gamma\gamma gg$ [22], 4γ [23], etc. These results are included in the constraints we considered.

As we checked, the main decay mode of the light scalar is usually to $b\bar{b}$ when $m_s \gtrsim 2m_b$. However, the color backgrounds at the LHC are very large; thus, a subleading Zh production process is used in detecting $h\to 2s\to 4b$, and VBF is used for $h\to 2s\to\gamma\gamma gg$. For the other decay mode, the main production process ggF can be used. Considering the cross sections of production and branching ratios of decay, as well as the detection precisions, we found that the detections in $4b$, $2b2\tau$, and $2\tau 2\mu$ channels are important for the scNMSSM. The signal rates are $\mu_{\rm Zh}\times Br(h\to ss\to 4b)$, $\mu_{\rm ggF}\times Br(h\to ss\to 2b2\tau)$, and $\mu_{\rm ggF}\times Br(h\to ss\to 2\tau 2\mu)$, respectively, where $\mu_{\rm ggF}$ and $\mu_{\rm Zh}$ are the ggF and Zh production rates normalized to their SM value, respectively [3-5][2)].

For detections of the exotic decay at the HL-LHC, we use the simulation results of 95% exclusion limit in Refs. [24,33]. Suppose, with an integrated luminosity of L_0, the 95% exclusion limit for branching ratio in some channel is Br_0 in the simulation result; then, for a sample in the model, if the signal rate is $\mu_i\times Br$ (i denotes the production channel), the signal significance with integrated luminosity of L will be

1) These indirect constraints on exotic branching ratios of the SM-like Higgs are complicated, since the signal event number depends on both corresponding cross sections and branching ratios of the Higgs boson. According to the combination of the global fit results, which we have considered in this work, the non-SM branching ratios of the SM-like Higgs is limited to 0 ~ 20%.

2) According to the combination of the global fit results, in SUSY models the reduced $h_{\rm SM}VV$ and reduced effective $h_{\rm SM}gg$ couplings are limited to 0.9 ~ 1.0 and 0.83 ~ 1.05 respectively. Thus $\mu_{\rm Zh}$ can only vary in the range 0.81 ~ 1.00, and the signal rates shown in Figs. 7-10 approach to the corresponding branching ratios of the SM-like Higgs decay to four light particles though a pair of light scalars.

$$ss = 2\,\frac{\mu_i \times Br}{Br_0}\sqrt{\frac{L}{L_0}}, \tag{30}$$

and the integrated luminosity needed to exclude the sample in the channel at 95% confidence level (with $ss = 2$) will be

$$L_{\rm e} = L_0\left(\frac{Br_0}{\mu_i \times Br}\right)^2, \tag{31}$$

and the integrated luminosity needed to discover the sample in the channel (with $ss = 5$) will be

$$L_{\rm d} = L_0\left(\frac{5}{2}\right)^2\left(\frac{Br_0}{\mu_i \times Br}\right)^2. \tag{32}$$

In Figs. 4, 5, and 6, we show the signal rates for the surviving samples in the three scenarios and the 95% exclusion bounds [24,33] in the $4b$, $2b2\tau$, and $2\tau2\mu$ channels, respectively. From these figures, one can see the following:

• With a light scalar heavier than 30 GeV, the easiest way to discover the exotic decay is via the $4b$ channel, and the minimal integrated luminosity needed to discover the decay in this channel can be 650 fb^{-1} for Scenario II.

• With a light scalar lighter than 20 GeV, the $2\tau2\mu$ channel can be important, especially for samples in Scenario II, and the minimal integrated luminosity needed to discover the decay in this channel can be 1000 fb^{-1}.

• With a light scalar heavier than $2m_b$, it is possible to discover the decay in the $2b2\tau$ channel, and the minimal integrated luminosity needed to discover the decay in this channel can be 1500 fb^{-1} for Scenario II.

B. Detections at the future lepton colliders

In future lepton colliders, such as CEPC, FCC-ee, and International Linear Collider (ILC), the main production process of the SM-like Higgs is Zh, and the color backgrounds are minimal; thus, these lepton colliders are powerful in detecting the exotic decay. There have been simulation results in many channels, such as $4b$, $4j$, $2b2\tau$, and 4τ [26]. With the same method as in the last subsection, one can perform similar analyses.

In Figs. 7, 8, 9, and 10, we show the signal rates for

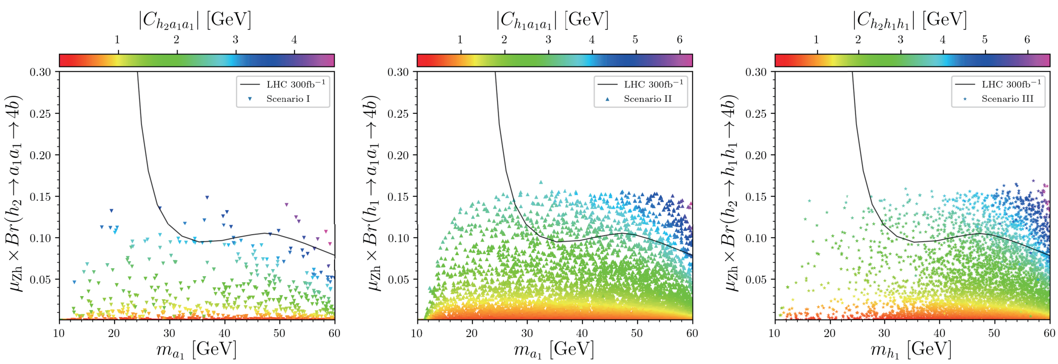

Fig. 4. (color online) Surviving samples for the three scenarios in the signal rate $\mu_{\rm Zh}\times Br(h\to ss\to 4b)$ versus the mass of light Higgs m_s planes, respectively, with colors indicating the tri-scalar coupling C_{hss} including one-loop correction, where h denotes the SM-like Higgs h_2 (left and right) and h_1 (middle), and s denotes the light scalar a_1 (left and middle) and h_1 (right). The solid curves indicate the simulation results of the 95% exclusion limit in the corresponding channel at the HL-LHC with 300 fb^{-1} [33].

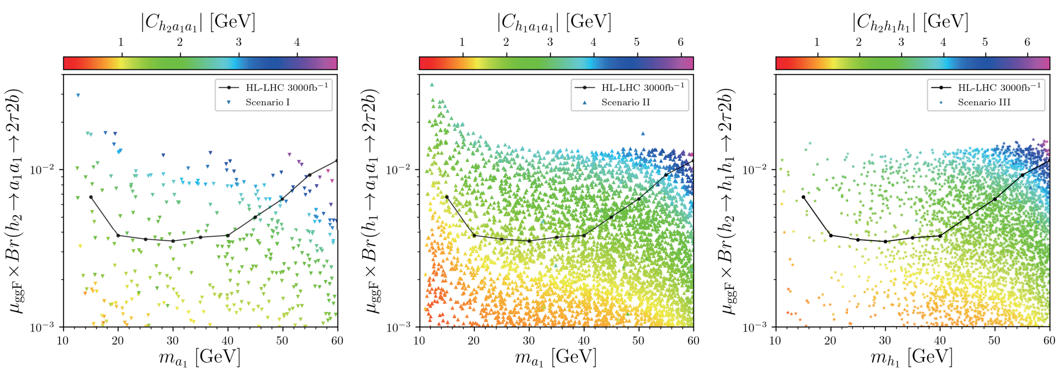

Fig. 5. (color online) Same as in Fig. 4, but shows the signal rate $\mu_{\rm ggF}\times Br(h\to ss\to 2\tau 2b)$ and 95% exclusion bounds in the corresponding channel at the HL-LHC with 3000 fb^{-1} [24].

surviving samples in the three scenarios and the 95% exclusion bounds (following the simulation results in Ref. [26]) at the CEPC, FCC-ee, and ILC, and in the $4b$, $4j$, $2b2\tau$, and 4τ channels, respectively. In these processes, the backgrounds are mainly from SM Higgs decays to four light particles through SM gauge bosons. From these figures, one can see the following:

• As in Fig. 7, when the light scalar is heavier than approximately 15 GeV and the tri-scalar coupling is large enough, the branching ratio for the $4b$ channel is significant. The minimal integrated luminosity needed to discover the decay in this channel can be 0.31 fb^{-1} for Scenari-

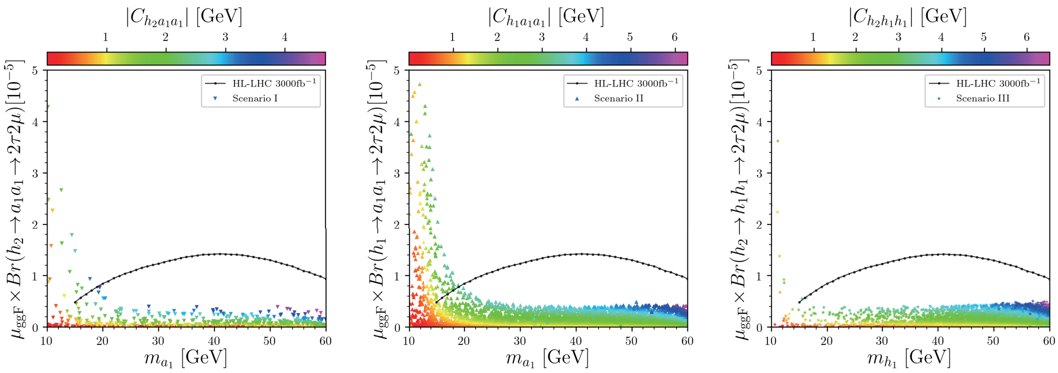

Fig. 6. (color online) Same as in Fig. 4, but shows the signal rate $\mu_{\rm ggF}\times Br(h\to ss\to 2\tau2\mu)$ and 95% exclusion bounds in the corresponding channel at the HL-LHC with 3000 fb^{-1} [24].

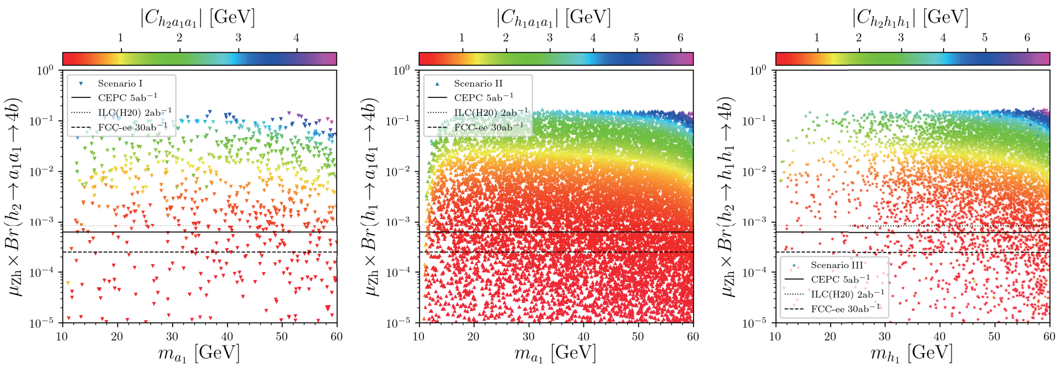

Fig. 7. (color online) Surviving samples for the three scenarios in the signal rate $\mu_{\rm Zh}\times Br(h\to ss\to 4b)$ versus the mass of light Higgs m_s planes, respectively, with colors indicating the tri-scalar coupling C_{hss} including one-loop correction, where h denotes the SM-like Higgs h_2 (left and right) and h_1 (middle), and s denotes the light scalar a_1 (left and middle) and h_1 (right). The solid, dashed, and dotted lines are the 95% exclusion bounds from simulations in the corresponding channel at the CEPC with 5 ab^{-1}, FCC-ee with 30 ab^{-1}, and ILC with 2 ab^{-1}, respectively [26].

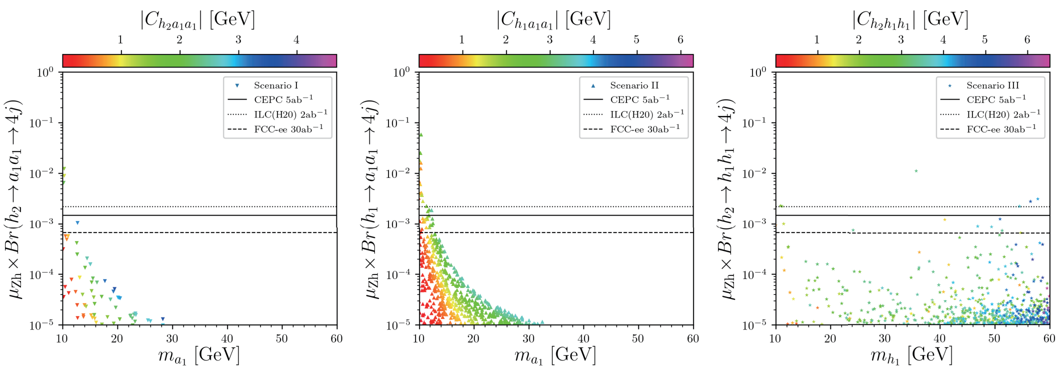

Fig. 8. (color online) Same as in Fig. 7, but shown are the signal rates $\mu_{\rm Zh}\times Br(h\to ss\to 4j)$ and 95% exclusion bounds in the corresponding channel [26]. The "$4j$" denotes four jets, including gluon and light quarks, except for b.

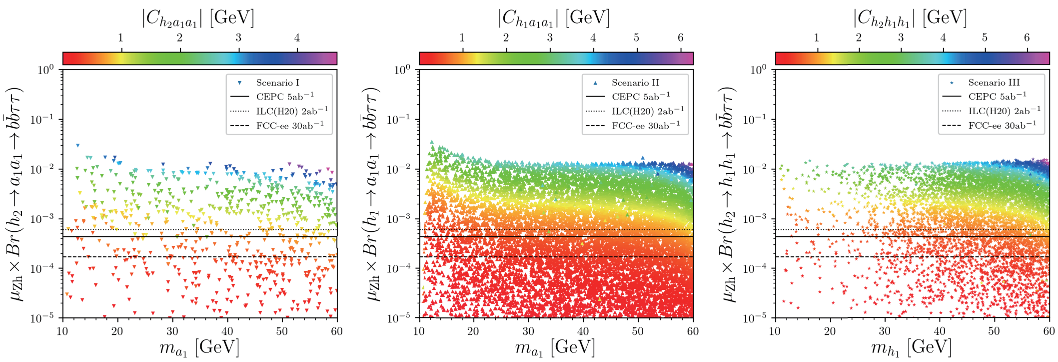

Fig. 9. (color online) Same as in Fig. 7, but shown are the signal rates $\mu_{\rm Zh}\times Br(h\to ss\to 2b2\tau)$ and 95% exclusion bounds in the corresponding channel [26].

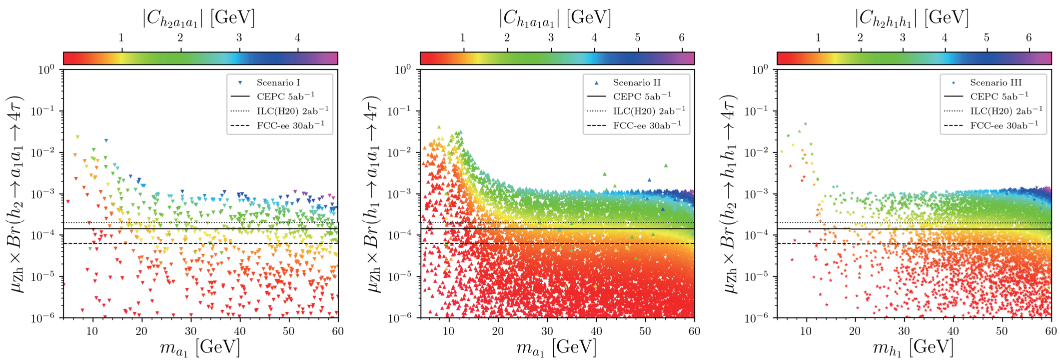

Fig. 10. (color online) Same as in Fig. 7, but shown are the signal rates $\mu_{\rm Zh}\times Br(h\to ss\to 4\tau)$ and 95% exclusion bounds in the corresponding channel [26].

os II and III at the ILC.

• As in Fig. 8, for Scenarios I and II, the exotic Higgs decay can be expected to be observed in the $4j$ channel when its mass is lighter than 11 GeV, whereas for Scenario III, the light scalar available at the CEPC can be as heavy as 40 GeV. The minimal integrated luminosity needed to discover the exotic decay in this channel can be 18 fb^{-1} for Scenario II at the ILC.

• As in Figs. 9 and 10, the signal rates in $2b2\tau$ and 4τ channel show similar trends. The branching ratios are small before the light scalar reaches the mass threshold, and the maximum values of branching ratios occur around $m_s=12$ GeV; the minimal integrated luminosity needed to discover the decay in the $2b2\tau$ channel is 3.6 fb^{-1} for Scenario II at the ILC, and that in the 4τ channel is 0.22 fb^{-1} for Scenario III at the ILC.

IV. CONCLUSIONS

In this work, we have discussed the exotic Higgs decay to a pair of light scalars in the scNMSSM, or the NMSSM with NUHM. First, we performed a general scan over the nine-dimension parameter space of the scNMSSM, considering the theoretical constraints of vacuum stability and Landau pole as well as experimental constraints of Higgs data, non-SM Higgs searches, muon g-2, sparticle searches, relic density and direct searches for dark matter, etc. Then, we found three scenarios with a light scalar of $10\sim60$ GeV: (i) the light scalar is CP-odd, and the SM-like Higgs is h_2; (ii) the light scalar is CP-odd, and the SM-like Higgs is h_1; and (iii) the light scalar is CP-even, and the SM-like Higgs is h_2. For the three scenarios, we check the parameter regions that lead to the scenarios, the mixing levels of the doublets and singlets, the tri-scalar coupling between the SM-like Higgs and a pair of light scalars, the branching ratio of Higgs decay to the light scalars, and the detections at the hadron colliders and future lepton colliders.

In this work, we compare the three scenarios, checking the interesting parameter regions that lead to the scenarios, the mixing levels of the doublets and singlets, the tri-scalar coupling between the SM-like Higgs and a pair of light scalars, the branching ratio of Higgs decay to the light scalars, and the detections at the hadron colliders and future lepton colliders.

Finally, we draw the following conclusions regarding a light scalar and the exotic Higgs decay to a pair of it in the scNMSSM:

• There are different interesting mechanisms in the three scenarios to tune parameters to obtain the small tri-scalar couplings.

• The singlet components of the SM-like Higgs in the

Table 2. The minimum integrated luminosity for discovering (at 5σ level) the exotic Higgs decay at the future colliders, where "@I, II, III" indicates the three different scenarios.

Decay Mode	Futrue colliders			
	HL-LHC	CEPC	FCC-*ee*	ILC
$(b\bar{b})(b\bar{b})$	650 fb^{-1}(@II)	0.42 fb^{-1}(@III)	0.41 fb^{-1}(@III)	0.31 fb^{-1}(@II)
$(jj)(jj)$	–	21 fb^{-1}(@II)	18 fb^{-1}(@II)	25 fb^{-1}(@II)
$(\tau^+\tau^-)(\tau^+\tau^-)$	–	0.26 fb^{-1}(@III)	0.22 fb^{-1}(@III)	0.31 fb^{-1}(@III)
$(b\bar{b})(\tau^+\tau^-)$	1500 fb^{-1}(@II)	4.6 fb^{-1}(@II)	3.6 fb^{-1}(@II)	4.4 fb^{-1}(@II)
$(\mu^+\mu^-)(\tau^+\tau^-)$	1000 fb^{-1}(@II)	–	–	–

three scenarios are at the same level of $\lesssim 0.3$ and are roughly one order of magnitude larger than the doublet component of the light scalar in Scenario I and II.

• The couplings between the SM-like Higgs and a pair of light scalars at tree level are $-3\sim5$, $-1\sim6$, and $-10\sim5$ GeV for Scenario I, II, and III, respectively.

• The stop-loop correction to the tri-scalar coupling in Scenario III can be a few GeV, much larger than those in Scenarios I and II.

• The most effective way to discover the exotic decay at the future lepton collider is via the 4τ channel, while that at the HL-LHC is via the $4b$ channel for a light scalar heavier than 30 GeV and via $2b2\tau$ or $2\tau2\mu$ channel for a lighter scalar.

The details of the minimal integrated luminosity needed to discover the exotic Higgs decay at the HL-LHC, CEPC, FCC-ee, and ILC are summarized in Table 2, and the tuning mechanisms in the three scenarios to obtain the small tri-scalar coupling can be seen from Figs. 1,2 and Eqs. (17)-(26).

References

[1] G. Aad *et al.* (ATLAS), Phys. Lett. B **716**, 1-29 (2012), arXiv:1207.7214[hep-ex]

[2] S. Chatrchyan *et al.* (CMS), Phys. Lett. B **716**, 30-61 (2012), arXiv:1207.7235[hep-ex]

[3] G. Aad *et al.* (ATLAS and CMS), JHEP **08**, 045 (2016), arXiv:1606.02266[hep-ex]

[4] A. M. Sirunyan *et al.* (CMS), Eur. Phys. J. C **79**(5), 421 (2019), arXiv:1809.10733[hep-ex]

[5] G. Aad *et al.* (ATLAS), Phys. Rev. D **101**(1), 012002 (2020), arXiv:1909.02845[hep-ex]

[6] [CMS], CMS-PAS-HIG-19-005

[7] A. Sopczak (ATLAS and CMS), PoS **FFK2019**, 006 (2020), arXiv:2001.05927[hep-ex]

[8] R. Barate *et al.* (LEP Working Group for Higgs boson searches, ALEPH, DELPHI, L3 and OPAL), Phys. Lett. B **565**, 61-75 (2003), arXiv:hep-ex/0306033[hep-ex]

[9] A. M. Sirunyan *et al.* (CMS), JHEP **11**, 161 (2018), arXiv:1808.01890[hep-ex]

[10] [ATLAS], ATLAS-CONF-2019-036

[11] A. M. Sirunyan *et al.* (CMS), Phys. Lett. B **785**, 462 (2018), arXiv:1805.10191[hep-ex]

[12] M. Aaboud *et al.* (ATLAS), Phys. Lett. B **790**, 1-21 (2019), arXiv:1807.00539[hep-ex]

[13] A. M. Sirunyan *et al.* (CMS), Phys. Lett. B **795**, 398-423 (2019), arXiv:1812.06359[hep-ex]

[14] A. M. Sirunyan *et al.* (CMS), JHEP **08**, 139 (2020), arXiv:2005.08694[hep-ex]

[15] A. M. Sirunyan *et al.* (CMS), JHEP **11**, 018 (2018), arXiv:1805.04865[hep-ex]

[16] A. M. Sirunyan *et al.* (CMS), Phys. Lett. B **800**, 135087 (2020), arXiv:1907.07235[hep-ex]

[17] V. Khachatryan *et al.* (CMS), JHEP **10**, 076 (2017), arXiv:1701.02032[hep-ex]

[18] [CMS], CMS-PAS-HIG-16-035.

[19] [CMS], CMS-PAS-HIG-18-003.

[20] M. Aaboud *et al.* (ATLAS), JHEP **06**, 166 (2018), arXiv:1802.03388[hep-ex]

[21] M. Aaboud *et al.* (ATLAS), JHEP **10**, 031 (2018), arXiv:1806.07355[hep-ex]

[22] M. Aaboud *et al.* (ATLAS), Phys. Lett. B **782**, 750-767 (2018), arXiv:1803.11145[hep-ex]

[23] [ATLAS], ATLAS-CONF-2012-079

[24] [CMS], CMS-PAS-FTR-18-035

[25] F. An, Y. Bai, C. Chen *et al.*, Chin. Phys. C **43**(4), 043002 (2019), arXiv:1810.09037[hep-ex]

[26] Z. Liu, L. T. Wang, and H. Zhang, Chin. Phys. C **41**(6), 063102 (2017), arXiv:1612.09284[hep-ph]

[27] D. Curtin, R. Essig, S. Gori *et al.*, Phys. Rev. D **90**(7), 075004 (2014), arXiv:1312.4992[hep-ph]

[28] R. Dermisek and J. F. Gunion, Phys. Rev. D **73**, 111701 (2006), arXiv:hep-ph/0510322[hep-ph]

[29] R. Dermisek and J. F. Gunion, Phys. Rev. D **75**, 075019 (2007), arXiv:hep-ph/0611142[hep-ph]

[30] R. Dermisek, J. F. Gunion, and B. McElrath, Phys. Rev. D **76**, 051105 (2007), arXiv:hep-ph/0612031[hep-ph]

[31] M. Carena, T. Han, G. Y. Huang *et al.*, JHEP **04**, 092 (2008), arXiv:0712.2466[hep-ph]

[32] K. Cheung, J. Song, and Q. S. Yan, Phys. Rev. Lett. **99**, 031801 (2007), arXiv:hep-ph/0703149[hep-ph]

[33] J. Cao, F. Ding, and C. Han , JHEP **11**, 018 (2013), arXiv:1309.4939[hep-ph]

[34] X. F. Han, L. Wang, J. M. Yang *et al.*, Phys. Rev. D **87**(5), 055004 (2013), arXiv:1301.0090[hep-ph]

[35] J. Cao, Y. He, P. Wu *et al.*, JHEP **01**, 150 (2014), arXiv:1311.6661[hep-ph]

[36] L. Liu, H. Qiao, K. Wang *et al.*, Chin. Phys. C **43**(2), 023104 (2019), arXiv:1812.00107[hep-ph]

[37] L. Wang, X. F. Han, and B. Zhu, Phys. Rev. D **98**(3), 035024 (2018), arXiv:1801.08317[hep-ph]

[38] E. J. Chun, S. Dwivedi, T. Mondal *et al.*, Phys. Lett. B **774**, 20-25 (2017), arXiv:1707.07928[hep-ph]

[39] J. Bernon, J. F. Gunion, Y. Jiang *et al.*, Phys. Rev. D **91**(7), 075019 (2015), arXiv:1412.3385[hep-ph]

[40] I. Engeln, M. Mühlleitner, and J. Wittbrodt, Comput. Phys.

Commun. **234**, 256-262 (2019), arXiv:1805.00966[hep-ph]
[41] U. Haisch, J. F. Kamenik, A. Malinauskas *et al*., JHEP **03**, 178 (2018), arXiv:1802.02156[hep-ph]
[42] S. Liu, Y. L. Tang, C. Zhang *et al*., Eur. Phys. J. C **77**(7), 457 (2017), arXiv:1608.08458[hep-ph]
[43] S. F. King, M. Mühlleitner, R. Nevzorov *et al*., Nucl. Phys. B **870**, 323-352 (2013), arXiv:1211.5074[hep-ph]
[44] R. Benbrik, M. Gomez Bock, S. Heinemeyer *et al*., Eur. Phys. J. C **72**, 2171 (2012), arXiv:1207.1096[hep-ph]
[45] J. J. Cao, Z. X. Heng, J. M. Yang *et al*., JHEP **03**, 086 (2012), arXiv:1202.5821[hep-ph]
[46] J. Cao, Z. Heng, J. M. Yang *et al*., JHEP **10**, 079 (2012), arXiv:1207.3698[hep-ph]
[47] Z. Kang, J. Li, and T. Li, JHEP **11**, 024 (2012), arXiv:1201.5305[hep-ph]
[48] S. F. King, M. Muhlleitner, and R. Nevzorov, Nucl. Phys. B **860**, 207-244 (2012), arXiv:1201.2671[hep-ph]
[49] U. Ellwanger, JHEP **03**, 044 (2012), arXiv:1112.3548[hep-ph]
[50] U. Ellwanger, A. Florent, and D. Zerwas, JHEP **01**, 103 (2011), arXiv:1011.0931[hep-ph]
[51] D. E. Lopez-Fogliani, L. Roszkowski, R. Ruiz de Austri *et al*., Phys. Rev. D **80**, 095013 (2009), arXiv:0906.4911[hep-ph]
[52] G. Belanger, C. Hugonie, and A. Pukhov, JCAP **01**, 023 (2009), arXiv:0811.3224[hep-ph]
[53] A. Djouadi, U. Ellwanger, and A. M. Teixeira, JHEP **04**, 031 (2009), arXiv:0811.2699[hep-ph]
[54] U. Ellwanger, AIP Conf. Proc. **1078**(1), 73-78 (2009), arXiv:0809.0779[hep-ph]
[55] C. Hugonie, G. Belanger, and A. Pukhov, JCAP **11**, 009 (2007), arXiv:0707.0628[hep-ph]
[56] K. Kowalska, S. Munir, L. Roszkowski *et al*., Phys. Rev. D **87**, 115010 (2013), arXiv:1211.1693[hep-ph]
[57] J. F. Gunion, Y. Jiang, and S. Kraml, Phys. Lett. B **710**, 454-459 (2012), arXiv:1201.0982[hep-ph]
[58] J. Cao, Z. Heng, D. Li *et al*., Phys. Lett. B **710**, 665-670 (2012), arXiv:1112.4391[hep-ph]
[59] J. Ellis and K. A. Olive, Eur. Phys. J. C **72**, 2005 (2012), arXiv:1202.3262[hep-ph]
[60] P. Bechtle, J. E. Camargo-Molina, K. Desch *et al*., Eur. Phys. J. C **76**(2), 96 (2016), arXiv:1508.05951[hep-ph]
[61] P. Athron *et al*. (GAMBIT), Eur. Phys. J. C **77**(12), 824 (2017), arXiv:1705.07935[hep-ph]
[62] F. Wang, K. Wang, J. M. Yang *et al*., JHEP **12**, 041 (2018), arXiv:1808.10851[hep-ph]
[63] D. Das, U. Ellwanger and A. M. Teixeira, JHEP **04**, 117 (2013), arXiv:1301.7584[hep-ph]
[64] U. Ellwanger and C. Hugonie, JHEP **08**, 046 (2014), arXiv:1405.6647[hep-ph]
[65] K. Wang, F. Wang, J. Zhu *et al*., Chin. Phys. C **42**(10), 103109-103109 (2018), arXiv:1811.04435[hep-ph]
[66] K. Nakamura and D. Nomura, Phys. Lett. B **746**, 396-405 (2015), arXiv:1501.05058[hep-ph]
[67] K. Wang and J. Zhu, JHEP **06**, 078 (2020), arXiv:2002.05554[hep-ph]
[68] K. Wang and J. Zhu, Phys. Rev. D **101**(9), 095028 (2020), arXiv:2003.01662[hep-ph]
[69] K. Wang and J. Zhu, Chin. Phys. C **44**(6), 061001 (2020), arXiv:1911.08319[hep-ph]
[70] U. Ellwanger and C. Hugonie, Eur. Phys. J. C **78**(9), 735 (2018), arXiv:1806.09478[hep-ph]
[71] U. Ellwanger, JHEP **02**, 051 (2017), arXiv:1612.06574[hep-ph]
[72] M. Maniatis, Int. J. Mod. Phys. A **25**, 3505-3602 (2010), arXiv:0906.0777[hep-ph]
[73] M. Carena, H. E. Haber, I. Low *et al*., Phys. Rev. D **93**(3), 035013 (2016), arXiv:1510.09137[hep-ph]
[74] U. Ellwanger, J. F. Gunion, and C. Hugonie, JHEP **02**, 066 (2005), arXiv:hep-ph/0406215[hep-ph]
[75] U. Ellwanger and C. Hugonie, Comput. Phys. Commun. **175**, 290-303 (2006), arXiv:hep-ph/0508022[hep-ph]
[76] P. Bechtle, O. Brein, S. Heinemeyer *et al*., Comput. Phys. Commun. **181**, 138-167 (2010), arXiv:0811.4169[hep-ph]
[77] P. Bechtle, O. Brein, S. Heinemeyer *et al*., Comput. Phys. Commun. **182**, 2605-2631 (2011), arXiv:1102.1898[hep-ph]
[78] P. Bechtle, O. Brein, S. Heinemeyer *et al*., Eur. Phys. J. C **74**(3), 2693 (2014), arXiv:1311.0055[hep-ph]
[79] A. M. Sirunyan *et al*. (CMS), JHEP **03**, 160 (2018), arXiv:1801.03957[hep-ex]
[80] M. Tanabashi *et al*. (Particle Data Group), Phys. Rev. D **98**(3), 030001 (2018)
[81] E. Aprile *et al*. (XENON), Phys. Rev. Lett. **121**(11), 111302 (2018), arXiv:1805.12562[astro-ph.CO]
[82] E. Aprile *et al*. (XENON), Phys. Rev. Lett. **122**(14), 141301 (2019), arXiv:1902.03234[astro-ph.CO]